



1 **Variability in individual particle structure and mixing**
2 **states between the glacier snowpack and atmosphere**
3 **interface in the northeast Tibetan Plateau**

4 Zhiwen Dong ^{a, b, *}, Shichang Kang ^{a, c}, Yaping Shao ^b, Sven Ulbrich ^b, Dahe Qin ^a

5 ^a State Key Laboratory of Cryosphere Sciences, Northwest Institute of Eco-Environment
6 and Resources, Chinese Academy of Sciences, Lanzhou 730000, China;

7 ^b Institute for Geophysics and Meteorology, University of Cologne, Cologne D-50923,
8 Germany;

9 ^c CAS Center for Excellence in Tibetan Plateau Earth Sciences, Beijing 100101, China.

10 * **Corresponding Author. E-mail Address:** dongzhiwen@lzb.ac.cn (Z. Dong).

11 **Abstract**

12 Aerosol impurities affect the earth's temperature and climate by altering the radiative
13 properties of the atmosphere. Changes in the composition, morphology structure and
14 mixing states of aerosol components will cause significantly varied radiative forcing in
15 the atmosphere. This work focused on the physicochemical properties of light-absorbing
16 impurities (LAIs) and their variability through deposition from the atmosphere to the
17 glacier/snowpack surface interface based on large-range observation in northeastern
18 Tibetan Plateau and laboratory transmission electron microscope (TEM) and laboratory
19 energy dispersive X-ray spectrometer (EDX) measurements. The results showed that LAI
20 particle structures changed markedly in the snowpack compared to those in the
21 atmosphere due to black carbon (BC)/organic matter (OM) particle aging and salt-coating
22 condition changes. Considerably more aged BC and OM particles were observed in
23 glacier/snowpack surfaces than in the atmosphere, as the proportion of aged BC and OM
24 varied in all locations by 4%-16% and 12%-25% in the atmosphere, respectively, whereas
25 they varied by 25%-36% and 36%-48%, respectively, in the glacier/snowpack surface.
26 Similarly, the salt-coated particle ratio of LAIs in the snowpack is lower than in the
27 atmosphere. Albedo change contribution in the Miaoergou, Yuzhufeng and Qiyi Glaciers



28 is evaluated using the SNICAR model for glacier surface distributed impurities. Due to
29 salt-coating state change, these values decreased by 30.1%-56.4% compared to that in the
30 atmosphere. Such great change may cause more strongly enhanced radiative heating than
31 previously thought, suggesting that the warming effect from particle structure and mixing
32 change of glacier/snowpack LAIs may have markedly affected the climate on a global
33 scale in terms of direct forcing in the cryosphere.

34 **Keywords:** light absorbing aerosols; atmosphere-snowpack interface; BC/OM particle
35 structure aging; salt-coating change; particle internal mixing

36 1. Introduction

37 Aerosols affect the earth's temperature and climate by altering the radiative properties of
38 the atmosphere (Jacobson, 2001; 2014). Snow cover and glaciers in cryospheric regions
39 play an important role in global climate change because of their large areas of distribution
40 on the earth's surface, especially in the Northern Hemisphere, e.g., in the Alpine
41 Mountains, the Tibetan Plateau, northern hemisphere snowpack and the Polar Regions.
42 Individual pollutant aerosols, e.g., black carbon (BC, or soot), organic carbon (OC) or
43 organic matter (OM), mineral dust and various salts, deposited on glacier/snowpack
44 surfaces cause enhanced surface heat absorption, acting as light absorbing impurities
45 (LAIs), and they thus impact radiative forcing in the cryosphere. Moreover, changes in
46 composition, morphology structure and mixing states of different LAIs components will
47 cause significant variability in individual particle radiative heating with largely varied
48 surface albedo due to the changes in a single particle's mixing states (Cappa et al., 2012;
49 Peng et al., 2016).

50 The Tibetan Plateau, acting as the "The Third Pole" region, is one of the largest
51 cryosphere regions with a large ice mass besides the Polar Regions (Qiu et al., 2008).
52 Large amounts of LAIs particles deposited on the glacier/snowpack surface can
53 significantly impact surface radiative forcing, and induce increased heat absorption of the
54 atmosphere interface in lower and middle troposphere (Anesio et al., 2009; Kaspari et al.,
55 2011; Dong et al., 2016, 2017), thereby causing rapid glacier melting in the region (Xu et
56 al., 2009; Zhang et al., 2017).



57 Aerosols and climate interaction has become a major concern in the Tibetan Plateau
58 region (Dong et al., 2016, 2017). For example, the long-range transport and deposition of
59 BC (soot), various types of salts (e.g., ammonium, nitrate and sulfate), and aerosols, and
60 their climate significance on the Tibetan Plateau glaciers have recently become heavily
61 researched topics (Ramanathan et al., 2007; Flanner et al., 2007; McConnell et al., 2007;
62 Zhang et al., 2018). However, to date, notably limited studies have focused on the
63 composition, mixing states, and change process of LAIs particles in the
64 atmosphere-snowpack interface of the Tibetan Plateau glacier basins. Moreover, current
65 modeling on cryospheric snow/ice radiative forcing's impact on climate change have
66 rarely considered such influences from changes to a single particle's structure and mixing
67 states (Ramanathan et al., 2007; Hu et al., 2018). Because of glacier ablation and LAI
68 accumulation in summer, the concentration of distributed impurities in glacier/snowpack
69 surface is often even higher than that of the atmosphere (Zhang et al., 2017; Yan et al.,
70 2016).

71 Therefore, this study aimed to provide a first and unique record of the individual LAIs
72 particle's physicochemical properties, components, composition, and mixing states of
73 LAIs between the glacier/snowpack and atmosphere interface over the northeastern
74 Tibetan Plateau based on aerosol sampling (TSP and microscope filter samples) and the
75 surface-distributed impurity samples of glaciers/snowpack, collected in the northeast
76 Tibetan Plateau from June 2016 to September 2017, to determine the individual LAIs
77 particle's structure aging and mixing state changes through the atmospheric deposition
78 process from atmosphere to glacier/snowpack surface, thereby helping to characterize the
79 LAIs' radiative forcing and climate effects in the cryosphere region of Tibetan Plateau.
80 Moreover, the albedo change contributions in several glacier surfaces (e.g., Miaoergou,
81 Yuzhufeng and Qiyi Glaciers) were evaluated using a SNICAR model for the salt mixing
82 states of surface- distributed impurities of the observed glaciers.

83 **2. Data and Methods**

84 The main methods of the study include fieldwork observations and laboratory
85 transmission electron microscope (TEM) and laboratory energy dispersive X-ray



86 spectrometer (EDX) instrument analysis. Atmospheric LAIs samples (including the
87 atmospheric TSP and TEM filter samples) and the glacier/snowpack surface distributed
88 impurity samples were both collected across the northeastern Tibetan Plateau region in
89 summer between June 2016 and September 2017. Figure 1 shows the sampling locations
90 and their spatial distribution in the region, including the Miaoergou Glacier (abbreviated
91 MG) in the eastern Tianshan Mountains; Laohugou Glacier No.12 (LG12), Qiyi Glacier
92 (QG), Lenglongling Glacier (LG), Shiyi Glacier (SG) and Dabanshan Snowpack (DS) in
93 the Qilian Mountains; Yuzhufeng Glacier (YG) in the Kunlun Mountains; the Gannan
94 snowpack (GS), Dagu Glacier (DG), and Hailuogou Glacier (HG) in the Hengduan
95 Mountains, where large-range observations were conducted (as shown in Table 1).
96 During the fieldwork sampling, we used the middle-volume-sampler (DKL-2 with a flow
97 rate of 150 L/min) for TEM filter sampling in this study. In total, 65 aerosol samples were
98 collected directly on the calcium-coated carbon (Ca-C) grid filter. Additionally, 88
99 glacier/snowpack surface samples were collected on the glacier/snowpack surface for
100 comparison with the deposition process. The detailed TEM sampling method is similar to
101 the previous study in Dong et al. (2017).

102 Laboratory TEM-EDX measurements were performed directly on the Ca-C filters grids
103 (Dong et al., 2016). Ca-C grids were used as filters with the advantage of clear and
104 unprecedented observation for single-particle analyses of aerosols and snowpack samples
105 (Creamean et al., 2013; Li et al, 2014; Semeniuk et al., 2014). Analyses of individual
106 particle observations were conducted using a JEM-2100F (JEOL) transmission electron
107 microscope operated at 200 kV. Detailed information of TEM-EDX measurements was
108 similar to that shown in our previous study (see Dong et al., 2016, 2017). In general,
109 more than 400 particles were analyzed per grid; thus, more than 1200 particles were
110 analyzed from the three grid fractions per sample. Moreover, as the snow samples'
111 melting will affect the individual particle composition during the measurements,
112 especially for various types of salts, the snow/aerosol samples were directly observed
113 under the TEM instrument and measured before it melted. Most samples were measured
114 in frozen states.

115 We also evaluated the albedo change contributed by individual particle mixing states'



116 variability of LAIs. The SNICAR model can be used to simulate the albedo of snowpack
117 by the combination of the impurity of the contents (e.g., BC, dust and volcanic ash), snow
118 effective grain size, and incident solar flux parameters (Flanner et al., 2007). Details for
119 running the SNICAR model are similar to that of Zhang et al. (2018). In the model
120 simulation, mineral dust (93.2 ug/g), BC (854 ug/g) and OC (974 ug/g) average
121 concentration data, as well as other parameters, such as effective grain size, snow density,
122 solar zenith angle, and snow depth on the glaciers, are considered, and mass absorption
123 cross-sections (MAC) for salt-coated BC is referred to the average situation derived from
124 the northern Tibetan Plateau glaciers (Zhang et al., 2017, 2018; Yan et al., 2016).

125 **3. Results and Discussion**

126 **3.1 Composition of Various LAIs Components between the Atmosphere and** 127 **Snowpack Interface in the Glacier Basins**

128 Figure 2 shows the component types of an individual haze particle in northwestern China.
129 Based on the above microscope observations, aerosols were classified into eight
130 components: NaCl salt, mineral dust, fly ash-BC (soot), sulfates, ammonium, nitrates,
131 and organic matter (OM). Figure 3 shows the comparison of individual LAIs particle
132 composition (e.g., mineral dust, BC, organic matter, sulfate and various salts) between
133 glacier/snowpack and atmosphere interface in northeast Tibetan Plateau region. We found
134 that the impurity components show large differences between the snowpack and
135 atmosphere in all locations, implying significant change through the aerosols' deposition
136 processing in the interface (Figure 3). LAIs components have a large change of
137 proportion in the interface, probably due to different atmospheric cleaning rates and
138 atmospheric processing with dry/wet aerosol deposition. Sulfates and other salts in the
139 atmosphere act as salt-coating forms to other particles with aggregated states and will be
140 dissolved and taken away with precipitating snow and meltwater in the snowpack, which
141 will cause reduced salt components (e.g., sulfate, nitrate, NaCl, and ammonium) in the
142 glacier/snowpack surface compared to those in the atmosphere. Therefore, we can
143 observe obvious changes in composition and mixing states of the impurities between the
144 atmosphere and glacier/snowpack surface in Figure 3, as the ratio of BC, organic matter,



145 and mineral dust components in the snowpack increased greatly during this process,
146 whereas the ratio of various salts in the snowpack decreased significantly (Figure 3).
147 Such change will undoubtedly cause a significant variability of impurities' heat absorbing
148 property in both the atmosphere and the glacier/snowpack surface. Meanwhile, the
149 deposition flux and processing of various types of aerosol particles are different, causing
150 the changes in composition and mixing states of impurities between the atmosphere and
151 cryosphere. Moreover, such aerosol change processes (especially through deposition with
152 precipitating snow) will also lead to large variability of individual LAIs particle
153 structures and morphology; for example, the particle's aging, salt-coating and mixing
154 states changes of BC and organic matter (internal or external mixing), as shown below,
155 which will cause further influences on the radiative forcing of the glacier/snowpack
156 surface.

157 **3.2 BC/OM Particle Structure Aging Variability between Atmosphere and** 158 **Snowpack Interface**

159 Figure 4 shows how the particle's structure changes during the individual particle aging
160 process when deposited from the atmosphere into the glacier snowpack surface. Figure
161 4a-4d is representative of that in atmosphere, whereas Figure 4e-4h is that in the
162 glacier/snowpack surface. It is clear that abundant aerosol particles were observed with
163 relatively fresh structure in the atmosphere, similar to previous studies (e.g., Li et al.,
164 2015; Peng et al., 2016). As shown in Figure 4a-4d, the fresh aerosol particles of BC and
165 OC (or organic matter, OM) appeared very common in the atmosphere as the main parts,
166 whereas as shown in Figure 4e-4h, more aged particles were found deposited in the
167 glacier/snowpack surface. This process is characterized by initial transformation from a
168 fractal structure to spherical morphology and the subsequent growth of fully compact
169 particles. Previous work has indicated the structure and mass absorption cross (MAC)
170 section change of BC particles in the atmosphere but has not discussed such change
171 phenomena of OM particles' change during the structure-aging process. This study
172 reveals clearly the structure and morphology change of BC and OM particles' structure
173 aging through the transport and deposition process to the glacier snowpack from the
174 atmosphere (Figure 4).



175 Based on TEM-EDX observations, we evaluated the aged BC/OM particle composition
176 ratio (%) in the snowpack and the atmosphere, respectively. Figure 5 shows the aging of
177 BC/OM individual particles and their composition ratio (%) change with the deposition
178 process from the atmosphere to the glacier/snowpack surface. The proportion of aged
179 BC/OM particles varied from 4%-16 % and 12%-25% in atmosphere, respectively, and
180 varied from 25%-36% and 36%-48% in the glacier/snowpack surface, respectively. The
181 amount of aged particles in snowpack is 2-3 times higher than that in the atmosphere. We
182 can demonstrate that in the atmosphere the BC/OM both showed high ratios of fresh
183 structure particles (fractal morphology), while in the glacier/snowpack surface more
184 particles indicated aged structure (spherical morphology), although there were a small
185 portion of particles still fresh (Figure 5). The change proportion of BC/OM particle aging
186 is very marked between the interfaces. Large amount of fresh particles varied to aged
187 particles throughout the deposition process between the transition at atmosphere and
188 glacier/snowpack interfaces (Figure 5). The particle structure is a very important factor
189 influencing radiative forcing as shown in previous studies (Peng et al., 2016); thus, such
190 changes in BC/OM particles' structure aging between the glacier snowpack and
191 atmosphere will actually influence the total radiative absorbing of the mountain
192 glacier/snowpack, even affecting that of the whole cryosphere on earth's surface.

193 **3.3 Changes in Salt-Coating Conditions and BC/OM Mixing States between the** 194 **Atmosphere and Snowpack Interface**

195 Using TEM-EDX microscope measurements, we can easily derive the salt-coating
196 conditions based on the advantage of the transmission micro-observation of the single
197 particle structure. In addition to particle structure aging, we find evident variability in
198 particle salt-coating conditions between the atmosphere and glacier/snowpack interface
199 during the observation period. Figure 6 demonstrates the different salt-coating examples
200 for individual aerosol particles (including BC, OM, and mineral dust) in the atmosphere
201 in various glacier basins in the northeast Tibetan Plateau. We found that the salt-coating
202 form is very common for impurity particles in the atmosphere, which will of course cause
203 significant influence on radiative forcing of the atmosphere. A large part of fresh BC/OM
204 (with fractal morphology) and mineral dust particles were coated by various salts, such as



205 sulfate, nitrates, and ammonium. Such obvious salt-coating conditions will cause reduced
206 atmospheric radiative forcing, due to the increase of albedo (IPCC, 2013).

207 Similarly, we also evaluated the salt-coated particle ratio for BC/OM and its change
208 between glacier/snowpack and atmosphere. Figure 7 shows the salt-coating proportion of
209 impurity particles and its difference between the glacier/snowpack and atmosphere
210 interface at those locations. The proportion of salt-coating particles varied largely from
211 the atmosphere to the glacier/snowpack surface (2-4 times more in the atmosphere than
212 that in snowpack). We can demonstrate that in the atmosphere impurity particles showed
213 higher ratios with salt coating, while in the snowpack, only a small part of them indicate
214 salt-coating. The change proportion of salt-coating particles is very marked, and this
215 change will cause very complicated changes in a particle's mixing states and structure, as
216 many particles without salt-coating will change to internally mixing with BC/OM
217 particles as a core, or external mixing with BC/OM, which will also significantly
218 influence the total radiative forcing (RF) of the mountain glaciers/snowpack in the
219 cryosphere.

220 Figure 8 shows the situation of internal mixing states of BC (soot), organic matter (OM)
221 and mineral dust particles in various glacier snowpacks in the region, which demonstrates
222 the influence of the transport and deposition process to a particle's structure change. Most
223 salts in the salt-coated particles will disappear when deposited into the glacier/snowpack
224 surface, and the mixing states change largely to the internal and external mixing forms
225 with BC/OM as the core, in which the internal mixing of BC and OM particles will cause
226 strongly enhanced radiative forcing as indicated in previous work (Jacobson et al., 2001).
227 The proportion change of an internally mixed BC particle with other particles is
228 presented in Figure 9, showing great increases in internal mixing after deposition among
229 the locations in the whole northeast Tibetan Plateau region. We find that with the
230 salt-dissolution, a large part of LAIs particles changed to the internally mixed BC/OM
231 particle with other aerosol particles. As a large number of particles lose the salt coating in
232 the snowpack compared with those in the atmosphere, the whole process will certainly
233 increase the heating absorption proportion of the LAIs. Moreover, as shown in Figure 10,
234 average conditions of single, internally and externally mixed BC/OM individual particles



235 in the glacier/snowpack of the northeast Tibetan Plateau changed greatly with the
236 diameter of the particle. With the increase in particle size, most BC/OM particles (PM>1
237 um) showed internal mixing conditions, which will influence the RF of the glacier
238 snowpack.

239 **3.4 Discussion of Particle Mixing States Variability and Its Contribution to** 240 **Radiative Forcing Enhancement**

241 Figure 11 shows the schematic diagram model for the explanation of the particle structure
242 aging and salt-coating changes, and a comparison of its influence to the radiative forcing
243 between the atmosphere and glacier/snowpack interface on the Tibetan Plateau. From the
244 above discussion, we find a large variability in LAIs particles' mixing forms between the
245 glacier/snowpack surface and atmosphere, mainly originating from the morphologic
246 changes of the LAIs particle's structure (e.g., aging of BC/OM), and salt-coating changes
247 from increased internal mixing of BC/OC particles. Moreover, due to glacier ablation and
248 accumulation of various types of impurities, the concentration of impurities in the
249 snowpack surface is often even higher than that of the atmosphere (Zhang et al., 2017;
250 Yan et al., 2016).

251 In general, as shown in Figure 11, (i) more fresh structure BC/OM particles were
252 observed in the atmosphere, whereas more aged BC/OM particles were found on the
253 glacier/snowpack surface. Aged BC/OM particles often mean stronger radiative forcing
254 in the snowpack than in the atmosphere (Peng et al., 2015). (ii) More salt-coated
255 particles were found in the atmosphere of the glacier basin, whereas reduced salt coating
256 was found in the glacier/snow surface. With thick salt coating, the LAIs' light- absorbing
257 properties may not be that much stronger than the particles without coating, as most salts
258 (sulfate, nitrates, ammonium and NaCl) did not have strong forcing because of their light-
259 absorbing property and hygroscopicity in the mixing states (IPCC, 2013; Li et al., 2014),
260 especially for sulfate/nitrate aggregated particles. (iii) With the salt-coating decrease,
261 more internally mixed particles of BC/OM surrounded by a well-mixed salt-shell were
262 observed from the individual particles of LAIs in the snow-ice of the cryospheric glacier
263 basin, when compared to that of the atmosphere. Internally mixed particles of BC/OM
264 have showed the strongest light absorption in previous modeling studies, as BC acts as a



265 cell-core with organic matter particles (also sometimes including some salts) surrounded.
266 In one study the mixing state was found to affect the BC global direct forcing by a factor
267 of 2.9 (0.27 Wm^{-2} for an external mixture, $+0.54 \text{ Wm}^{-2}$ for BC as a coated core, and
268 $+0.78 \text{ Wm}^{-2}$ for BC as well mixed internally), as shown in Cappa et al. (2012), Jacobson
269 et al. (2000, 2001) and He et al., 2015. (iv) In addition to the heat-absorbing from the
270 above particle structure change, the absorbing property of some components in the
271 atmosphere and cryosphere (snow and ice) also show a large variability, as most mineral
272 and OM (or OC) particles show negative radiative forcing in the atmosphere while
273 showing positive forcing in the glacier/snowpack surface, as indicated from IPCC AR5
274 (2013), Yan et al. (2016), Zhang et al. (2018), and Hu et al. (2018). Thus, the
275 heat-absorbing of LAIs as a whole will increase greatly in glacier/snowpack surface
276 environments.

277 Additionally, the extent of influence of such particle mixing state changes are also
278 important and need to be evaluated for radiative forcing. The SNICAR model is often
279 employed to simulate the hemispheric albedo of snow and ice for a unique combination
280 of LAIs contents (e.g., BC, dust, and volcanic ash), snow effective grain size, and
281 incident solar flux characteristics (Flanner et al., 2007). We also evaluated the influence
282 on albedo caused by individual particle structure and mixing state changes in the glaciers
283 of the northeast Tibetan Plateau region. As shown in Figure 12, the albedo changes in
284 MG, YG and LG12 is evaluated using the SNICAR model for glacier/snowpack surface-
285 distributed impurities, which decreased by 30.1%-56.4%, caused by salt-coating changes,
286 when compared to that of the hypothetical similar situation of glacier surface impurities'
287 composition as in the atmosphere.

288

289 **4. Conclusions**

290 The results showed that the impurities' particle structure changed greatly in snowpack
291 compared to that in the atmosphere, mainly due to particle aging (mainly BC and organic
292 matter), and the salt coating reduction process through the impurity particle's atmospheric
293 deposition. Many more aging BC and OM and more internally mixed BC particles were



294 observed in glacier snowpack than in the atmosphere during the simultaneous
295 observations; for example, the proportion of aged BC and OM varies from 4-16 % and
296 12-25% in the atmosphere respectively, and varies from 25-36% and 36-48% respectively
297 in the snowpack of the cryosphere. In addition to the heat absorbing from the above LAIs
298 particle structure change, the absorbing property of dust and OC in atmosphere and
299 cryosphere (snow and ice) also shows a large difference.

300 A schematic model diagram linking the explanation the LAIs' structure aging and
301 salt-coating change and comparing their influences to the radiative forcing between the
302 atmosphere and glacier snowpack was created in the study. Thus, the heat absorption of
303 the impurities as a whole will increase greatly in glacier snowpack environments.
304 Moreover, we also evaluated the increase in radiative forcing caused by LAIs particle
305 structures and mixing state changes. The albedo changes in MG, YG and LG12 were
306 evaluated using the SNICAR model simulation for distributed surface impurities in the
307 observed glaciers caused by salt coating changes, which decreased by 30.1%-56.4%
308 compared to glacier surface with similar conditions as in the atmosphere. We think the
309 modeling evaluation in this work is helpful in understanding the contribution of
310 individual particle structure and mixing change in atmosphere-snowpack interface.

311

312 **Acknowledgments**

313 This work was funded by the National Natural Science Foundation of China (41671062,
314 41721091), the State Key Laboratory of Cryosphere Sciences (SKLCS-ZZ-2018), and the
315 Youth Innovation Promotion Association, CAS (2015347). We also thank the field work
316 team (especially to Li G., Li Y. and Chen S.) in the northeast Tibetan Plateau for their
317 logistical work and sample collections. All the data used are contained within the paper
318 and tables, figures, and references.

319 **References**

320 China, S. et al., 2013. Morphology and mixing state of individual freshly emitted wildfire
321 carbonaceous particles. Nat. Commun. 4: 2122, doi: 10.1038/ncomms3122.



- 322 China, S., Scarnato, B., Owen, R. C., et al., 2015. Morphology and mixing state of aged
323 soot particles at a remote marine free troposphere site: Implications for optical properties,
324 *Geophys. Res. Lett.*, 42, 1243-1250, doi: 10.1002/2014gl062404.
- 325 Cappa, C.D., Onasch, T.B., Massoli, P., et al. 2012, Radiative Absorption Enhancements
326 Due to the Mixing State of Atmospheric Black Carbon, *Science*, 337, 1078-1081,
327 doi:10.1126/science.1223447.
- 328 Creamean, J.M., Suski, K.J., Rosenfeld, D., et al., 2013. Dust and Biological Aerosols
329 from the Sahara and Asia Influence Precipitation in the Western U.S. *Science* 339,
330 1572-1578. doi: 10.1126/science.1227279.
- 331 Dong Z., S. Kang, J. Guo et al., 2017. Composition and mixing states of brown haze
332 particle over the Himalayas along two transboundary south-north transects. *Atmospheric*
333 *Environment*, 156, 24-35. doi:10.1016/j.atmosenv. 2017.02.029.
- 334 Dong Z., Qin D., Kang S. et al., 2016. Individual particles of cryoconite deposited on the
335 mountain glaciers of the Tibetan Plateau: Insights into chemical composition and sources.
336 *Atmospheric Environment*, 138, 114-124. doi: 10.1016/j.atmosenv. 2016.05.020
- 337 Flanner, M. G., Zender, C. S., Randerson, J. T. & Rasch, P. J., 2007. Present-day climate
338 forcing and response from black carbon in snow. *J. Geophys. Res. Atmos.* 112, D11202.
- 339 He C., K.N. Liou, Y. Takano., et al., 2015, Variation of the radiative properties during
340 black carbon aging: theoretical and experimental intercomparison. *Atmos. Chem. Phys.*,
341 15, 11967–11980.
- 342 He, C., Li, Q. B., Liou, K. N., et al. 2014. Black carbon radiative forcing over the Tibetan
343 Plateau, *Geophys. Res. Lett.*, 41, 7806–7813, doi: 10.1002/2014gl062191.
- 344 Hu Z., S. Kang, Fangping Yan, et al. 2018. Dissolved organic carbon fractionation
345 accelerates glacier-melting: A case study in the northern Tibetan Plateau. *Science of the*
346 *Total Environment*, 627, 579-585.
- 347 Li, W., Chen S., Xu Y., et al., 2015. Mixing state and sources of submicron regional
348 background aerosols in the northern Qinghai–Tibet Plateau and the influence of biomass
349 burning, *Atmos. Chem. Phys.*, 15, 13365–13376.



- 350 Li, W., Shao, L., Shi, Z., et al., 2014. Mixing state and hygroscopicity of dust and haze
351 particles before leaving Asian continent, *J. Geophys. Res.*, 119, 1044–1059.
- 352 Jacobson, M. Z., 2001. Strong radiative heating due to the mixing state of black carbon in
353 atmospheric aerosols, *Nature*, 409, 695-697, doi: 10.1038/35055518.
- 354 Jacobson, M. Z., 2014. Effects of biomass burning on climate, accounting for heat and
355 moisture fluxes, black and brown carbon, and cloud absorption effects, *J. Geophys. Res.*
356 *Atmos.*, 119, 8980-9002, doi: 10.1002/2014JD021861.
- 357 Martins, J. V., Artaxo, P., Liou, S. S., Reid, J. S., Hobbs, P. V., and Kaufman, Y. J.:
358 Effects of black carbon content, particle size, and mixing on light absorption by aerosols
359 from biomass burning in Brazil, *J. Geophys. Res. Atmos.*, 103, 32041–32050, doi:
360 10.1029/98jd02593, 1998.
- 361 Ramanathan, V., Ramana, M., Roberts, G., et al., 2007. Warming trends in Asia
362 amplified by brown cloud solar absorption. *Nature* 448, 575-578.
- 363 Peng J., Hu M., Guo S., 2016. Markedly enhanced absorption and direct radiative forcing
364 of black carbon under polluted urban environments. *PNAS*, www.pnas.org/cgi/doi/10.1073/pnas.1602310113.
- 365
- 366 Qiu, J., 2008. The third pole. *Nature* 454, 393-396. <http://dx.doi.org/10.1038/454393a>.
- 367 Yan F., S., Kang, C., Li, et al. 2016. Concentration, sources and light absorption
368 characteristics of dissolved organic carbon on a medium-sized valley glacier, northern
369 Tibetan Plateau, *The Cryosphere*, 10, 2611-2621.
- 370 Zhang Y., S. Kang, M. Sprenger, et al. 2018. Black carbon and mineral dust in snow
371 cover on the Tibetan Plateau. *The Cryosphere*, 12, 413–431.
- 372 Zhang, Y., et al. (2017), Light-absorbing impurities enhance glacier albedo reduction in
373 the southeastern Tibetan plateau, *J. Geophys. Res. Atmos.*, 122, doi:
374 10.1002/2016JD026397.
- 375
- 376



377

378 **Tables**

379

380 **Table 1. Sampling locations, sampling dates, and cryoconite-snow depth at mountain**
 381 **glaciers of the northeast Tibetan Plateau**

Sites	Glacier	Mountains	Locations	Altitude (m a.s.l.)	Sampling Date	Number Snow/Aero sols	Particles Calculated
MG	Miaoergou Glacier	Tianshan Mountains	42.59N,94.16E	3800-4200	12-13June 2017	8/6	>1200
LG12	Laohugou Glacier No.12	Qilian Mountains	39°20N, 96°34E	4300-4700	10-25July, 2016, 3-8June, 10-21 August 2017	20/16	>1200
QG	Qiyi Glacier	Qilian Mountains	39.14°N, 97.45°E	4200-4750	10-12June 2017 20-22August 2017	11/8	>1200
DS	Daban Snowpack	Daban Mountains	37.21°N,101.24°E	3500-3700	3-4June 2017	8/4	>1200
LG	Lenglongling Glacier	Qilian Mountains	37.51N,101.54E	3558-3990	5-7June 2017	12/5	>1200
SG	Shiyi Glacier	Qilian Mountains	38°21N, 99°88E	3900-4400	3-4June 2017	9/6	>1200
YG	Yuzhufeng Glacier	Kunlun Mountains	35.41N, 94.16E	4300-4720	12 June 2017	12/8	>1200
GS	Gannan Snowpack	Gannan Plateau	34.2N, 103.5E	2900-3200	4-8 May 2017 6-9August 2017	6/4	>1200
DG	Dagu Glacier	Hengduan Mountains	33N, 101E	3200-390	20-22 Sept 2017	2/3	>1200
HG	Hailuogou Glacier	Hengduan Mountains	31N,101E	2900-3500	11-12August 2017	6/4	>1200

382

383

384

385

386



387

388

389 **Figure Captions**

390 **Figure 1** Location map showing the sampled glaciers and snowpack in the northeast
391 Tibetan Plateau, including the Miaoergou Glacier (MG), Laohugou Glacier No.12
392 (LG12), Qiyi Glacier (QG), Lenglongling Glacier (LG), Shiyi Glacier (SG), Dabanshan
393 snowpack (DS), Yuzhufeng Glacier (YG), Gannan Snowpack (GS), Dagu Glacier (DG),
394 and Hailuogou Glacier (HG), where large-range field observations of atmosphere and
395 glacier surface impurities were conducted.

396 **Figure 2** Component types of individual haze particles in northwest China. Based on the
397 above microscope observation, aerosols were classified into seven components: NaCl salt,
398 mineral dust, fly ash, BC (soot), sulfates, nitrates, and organic matter (OM).

399 **Figure 3** Comparison of individual particles' compositions of light-absorbing impurities
400 in the (a) atmosphere and (b) snow and ice surface of the glacier basin in Tibetan Plateau,
401 and (c) a photo of snowpack and glaciers in the Qilian Mountains taken from flight in
402 autumn 2017, showing large distribution of snow cover and glaciers in the north Tibetan
403 Plateau region -round.

404 **Figure 4** Structure change during the aging of individual black carbon (BC) / organic
405 matter (OM) particles when deposited from the atmosphere onto snow and ice surface.
406 Figures 3a-3d is representative of atmosphere, while Figure 3e-3h shows the condition of
407 snow and ice.

408 **Figure 5** Structure aging of BC/OC individual impurity particles and composition ratio
409 (%) change during the deposition process from the atmosphere to glacier snowpack

410 **Figure 6** Examples of different salt-coating conditions of BC, OM and dust for individual
411 particles in the atmosphere of various glacier basins in northeast Tibetan Plateau

412 **Figure 7** Salt-coating proportion changes of individual impurity particles between glacier
413 snowpack and atmosphere in various locations of northeast Tibetan Plateau



414 **Figure 8** Internal mixing states of BC (soot), OM and mineral dust particles, in the
415 various glacier snowpack in northeast Tibetan Plateau

416 **Figure 9** The proportion change of internally mixed BC particle with other particles,
417 showing the obvious increase of internally mixed BC/OM in glacier snowpack compared
418 with those in the atmosphere

419 **Figure 10** Average conditions of single, internally and externally mixed BC/OM
420 individual particles in the snowpack of northeast Tibetan Plateau glaciers, showing most
421 of the BC/OM with diameter $>1 \mu\text{m}$ in internally mixing conditions.

422 **Figure 11** Schematic diagram linking aging and salt coating change and comparing its
423 influence to the radiative forcing between the atmosphere and snowpack of a remote
424 glacier basin, causing markedly enhanced radiative heat absorption.

425 **Figure 12** Evaluation of snow albedo change of BC-salt coating change in the snowpack
426 compared with atmosphere using SNICAR model simulation in the MG (a, b), YG (c, d),
427 LG 12 (e, f), which shows the largely decreased albedo of snow surface impurities in
428 snowpack compared to that of the atmosphere, implying markedly enhanced radiative
429 forcing in the snowpack surface impurities.

430

431

432

433

434

435

436

437

438

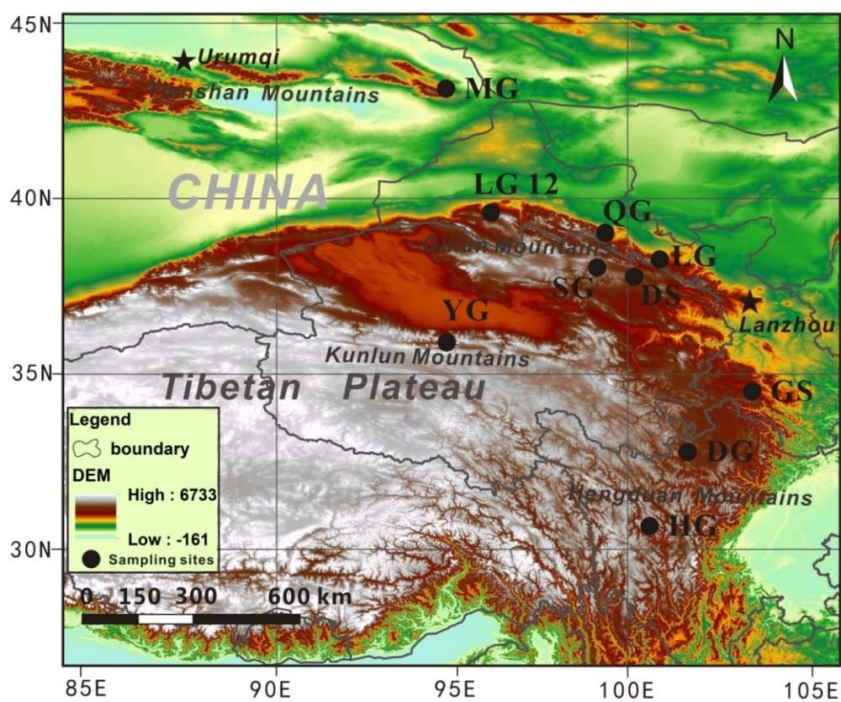


439

440

441 **Figure 1**

442



443

444

445

446

447

448

449

450

451

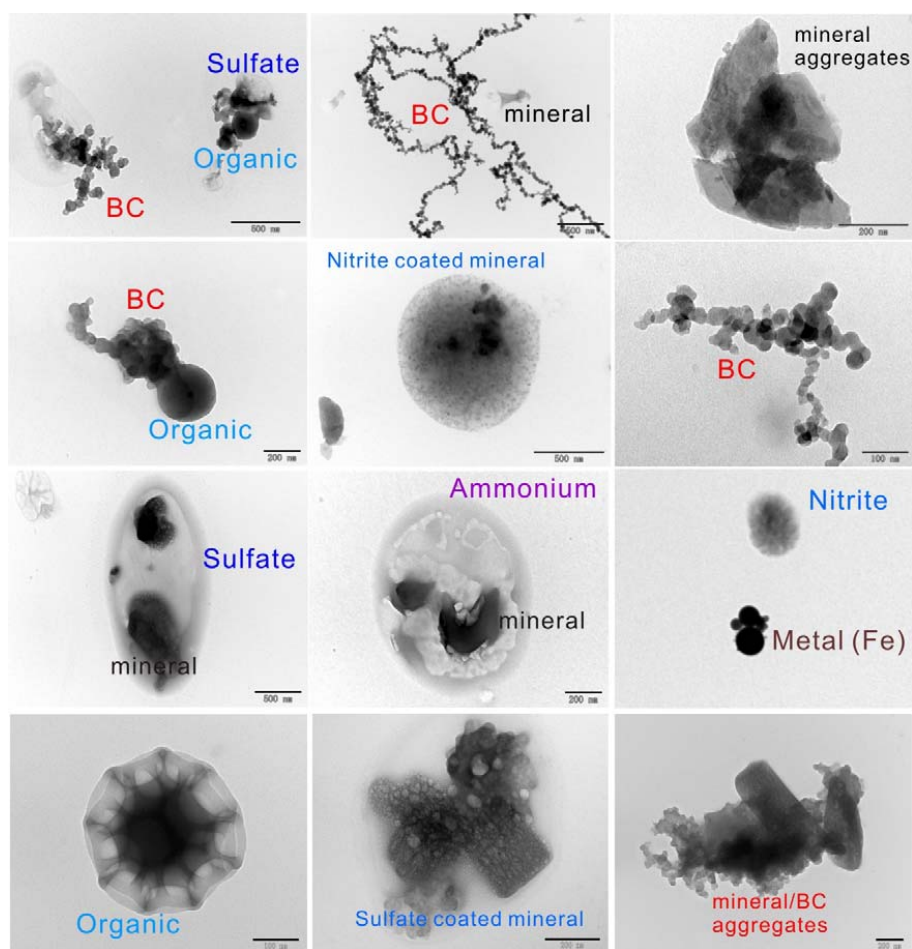


452

453

454

455 **Figure 2**



456

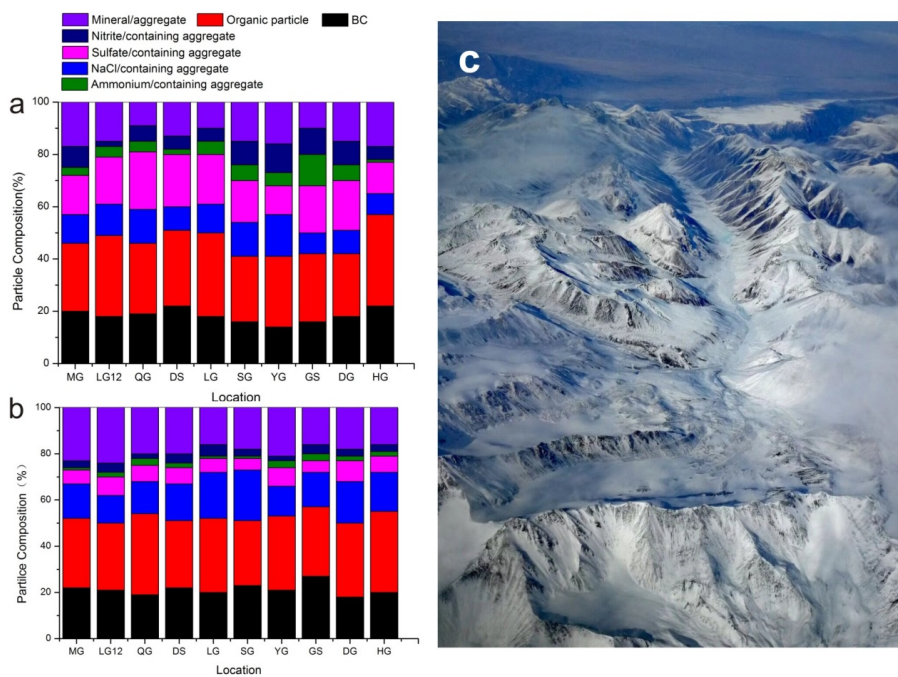
457

458

459



460 **Figure 3**

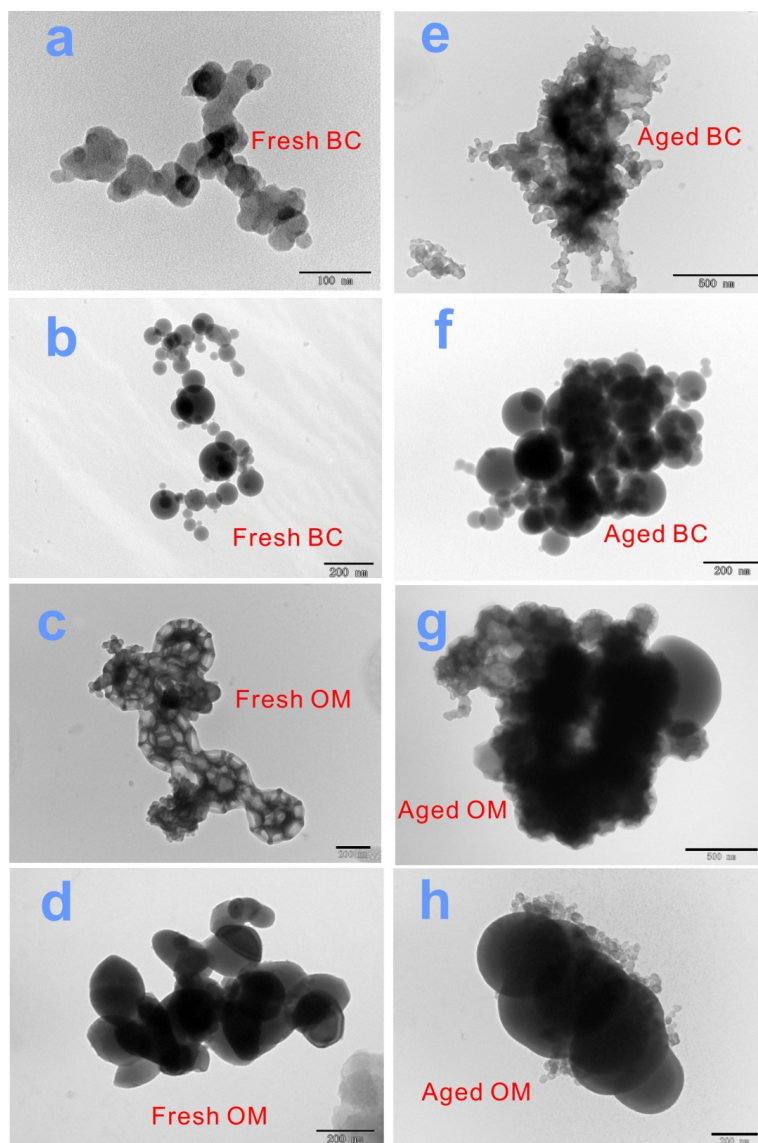


461
462
463
464
465
466
467
468
469
470



471

472 **Figure 4**

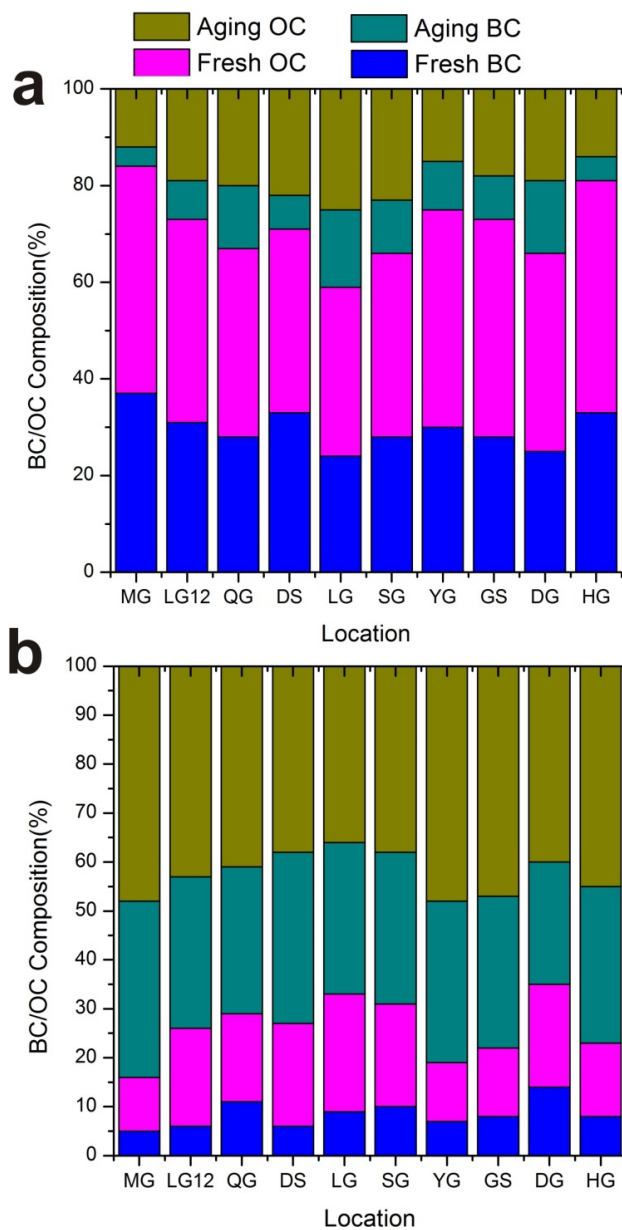


473

474



475 **Figure 5**



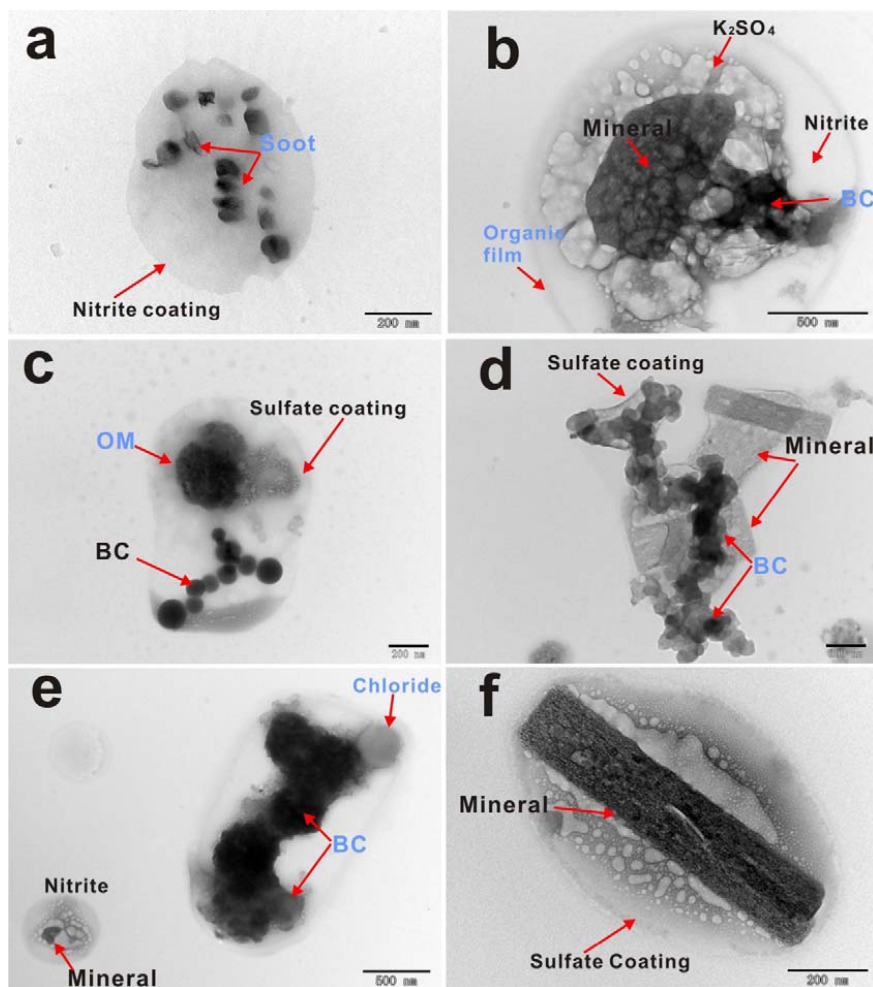
476

477



478

479 **Figure 6**



480

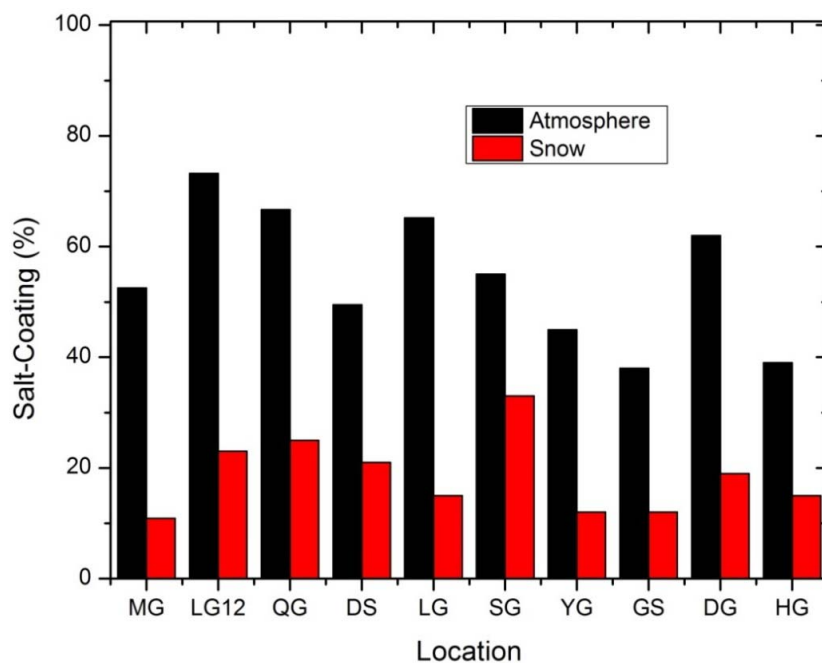
481

482

483



484 **Figure 7**



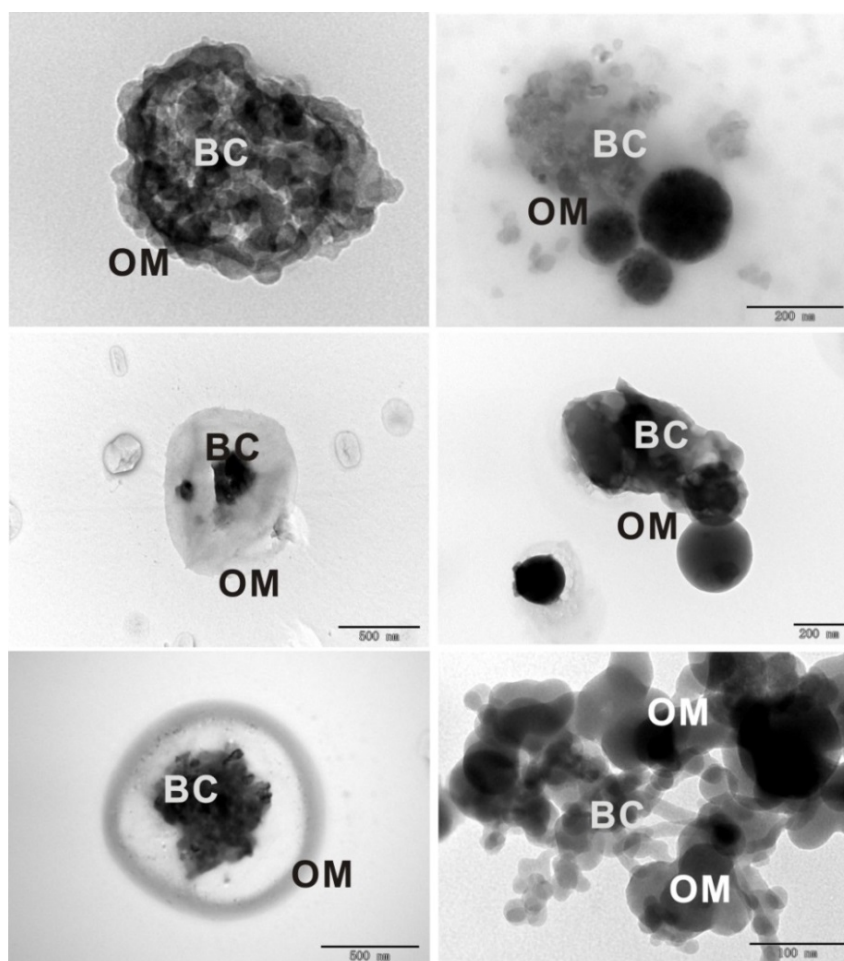
485
486
487
488
489
490
491
492
493
494
495
496
497



498

499 **Figure 8**

500



501

502

503

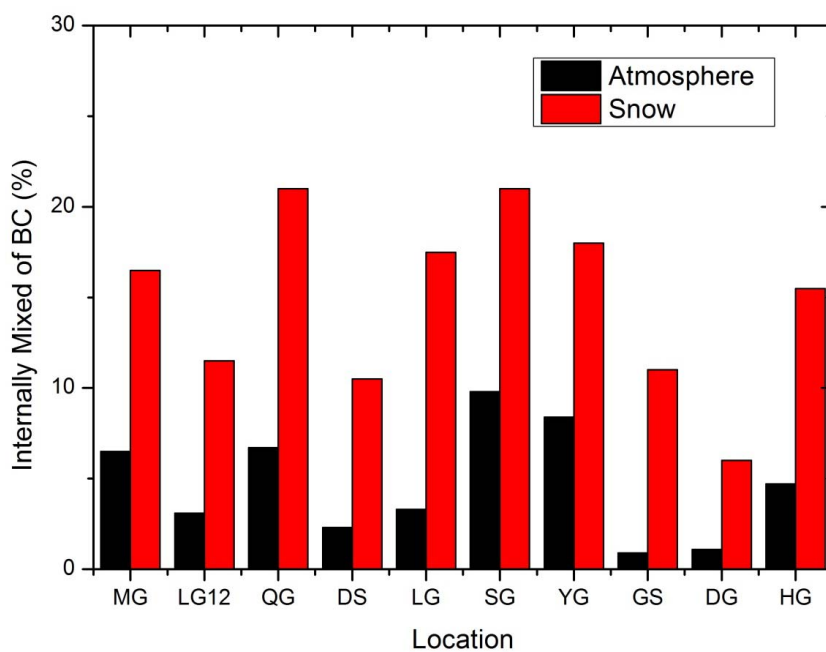
504



505

506 **Figure 9**

507



508

509

510

511

512

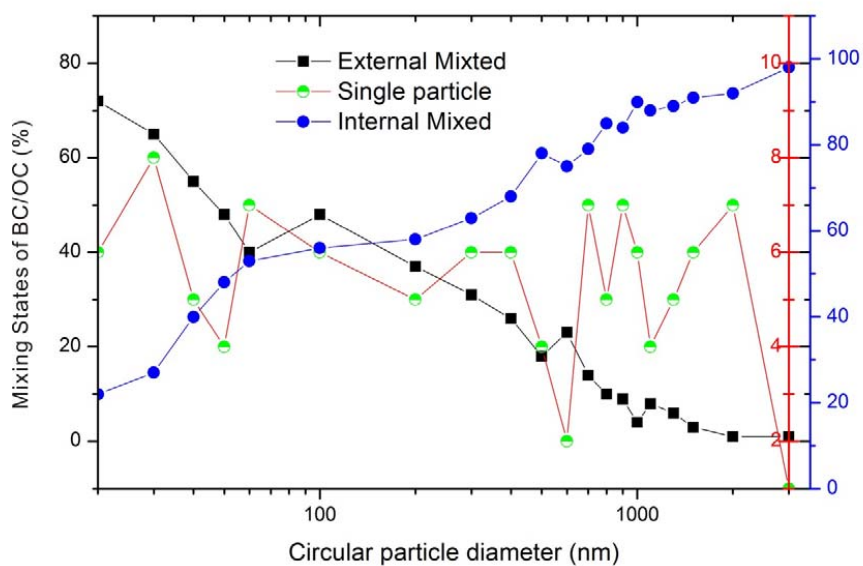
513

514



515

516 **Figure 10**



517

518

519

520

521

522

523

524

525

526

527

528

529

530



531

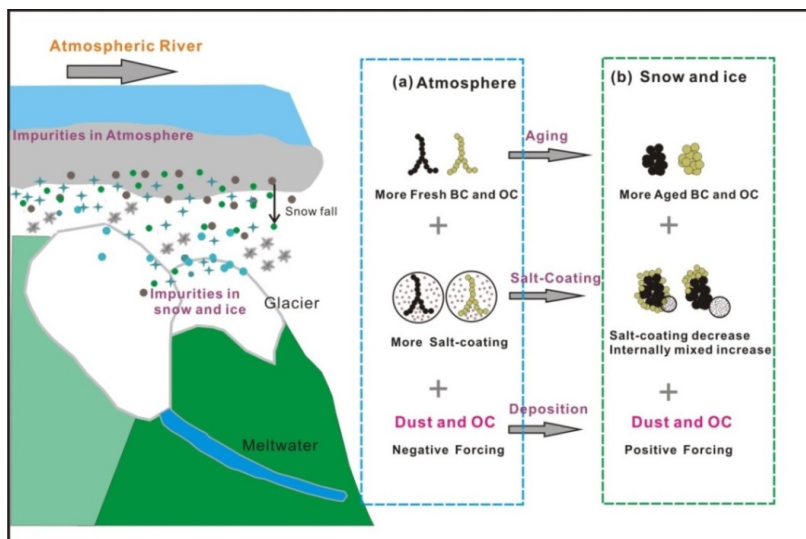
532

533

534

535

536 **Figure 11**



537

538

539

540

541

542

543

544

545

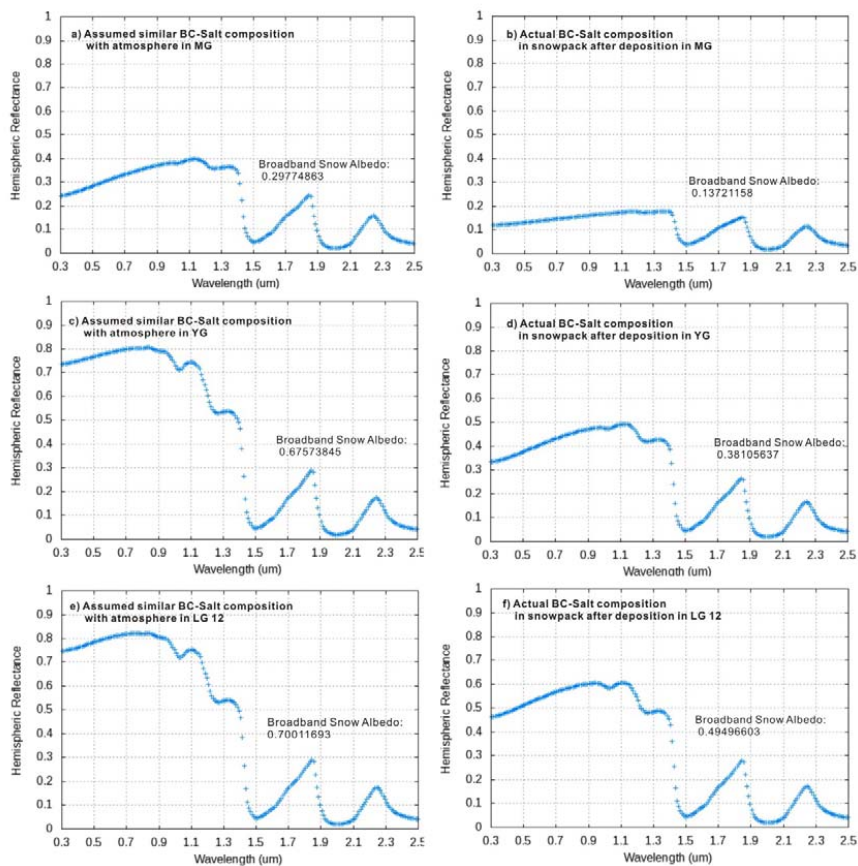
546

547



548

549 **Figure 12**



550

551

552